



A neural network model for the numerical prediction of the diameter of electro-spun polyethylene oxide nanofibers

Kamal Sarkar^{a,*}, Mounir Ben Ghalia^b, Zhenhua Wu^c, Subhash C. Bose^c

^a Department of Mechanical Engineering, The University of Texas-Pan American, Edinburg, TX 78541-2999, United States

^b Department of Electrical Engineering, The University of Texas-Pan American, Edinburg, TX 78541-2999, United States

^c Department of Manufacturing Engineering, The University of Texas-Pan American, Edinburg, TX 78541-2999, United States

ARTICLE INFO

Article history:

Received 29 November 2007

Received in revised form 8 June 2008

Accepted 13 July 2008

Keywords:

Electrospinning
Neural networks
Fiber diameter
Prediction

ABSTRACT

This paper investigates the viability of neural network as a tool for predicting the diameter of fiber formed by an electrospinning process. Published experimental data for polyethylene oxide (PEO) aqueous solution is used to train and test the neural network model. Concentration, conductivity, flow rate, and electric field strength are used as the input variables to the neural network model. Network model selection, training and testing were conducted using the k-fold cross validation technique which is demonstrated to be the most suitable scheme for the size of dataset used in this study. A statistical study was conducted to establish 95% confidence intervals on the bias and on the limits of agreement between the experimental data and the predicted data. The computer simulation results show a very good agreement between the data, demonstrating the viability of neural network as a promising tool for predicting fiber diameter. While the proposed neural network approach is not intended to model the complete complex physics of the electrospinning process, it is demonstrated to provide an accurate nonlinear mapping between the four salient input variables and the diameter of the formed fiber. This study provides some potential insights into exploring neural network model-based feedback control techniques to regulate nanofiber diameter in an electrospinning process.

© 2008 Elsevier B.V. All rights reserved.

1. Introduction

Electrospinning (Fig. 1) is a commonly used process to manufacture polymeric nanofibers (Reneker and Fong, 2006). In this process, a polymeric jet is driven through high voltage electric field that renders a typical meso-scale fluid jet into nano-scale fibers. Development of the electrospinning process can be traced back to more than a hundred years when Cooley and Morton discovered this phenomenon in 1902. Taylor initiated the first detailed mathematical study on this subject of electrified fluid jet in 1960s when he introduced the

“Leaky Dielectric Model” (Taylor, 1964, 1966, 1969; Melcher and Taylor, 1969). This model suggests that most of the charges for this class of dielectric accumulate only on the surface and not in the bulk fluid. Consequently, these fluids contain a nonzero electrical field tangent to the interface of the fluids. This nonzero electrical field causes a nonzero tangential stress on the interface that is balanced by the tangential viscous force of the fluid. Under these conditions the fluid will be in dynamic equilibrium. This model has been successfully used to compare the experimental results of neutrally buoyant drops elongated by an electric field. The resulting

* Corresponding author. Tel.: +1 956 381 2682; fax: +1 956 381 3527.

E-mail address: ksarkar@utpa.edu (K. Sarkar).

0924-0136/\$ – see front matter © 2008 Elsevier B.V. All rights reserved.

doi:10.1016/j.jmatprotec.2008.07.032

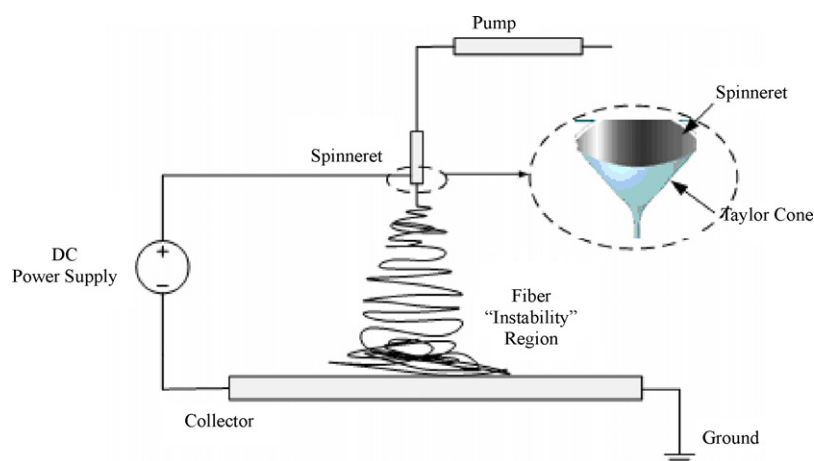


Fig. 1 – Illustration of electrospinning process.

fluid shape is the well known “Taylor Cone,” as illustrated in Fig. 1.

Based on Taylor’s work, Saville made a detailed discussion and derivation of the assumptions for the Taylor’s leaky dielectric model (Saville, 1997). In the seventies, he developed a linear stability model of an uncharged jet under the electrical field (Saville, 1970, 1971). His qualitative analysis on the characteristics of electrospinning is consistent with the experiments. He identified the presence of experimentally observed axisymmetric and oscillatory “whipping” instability of the centerline of the electrospinning jet. In subsequent research in electrospinning during the nineties, Reneker et al. (2000) and Fong et al. (1999) studied bending instability of the electrospinning process. They further identified the influence of solution properties on the formation of electrically charged jets (Fong et al., 1999). These include viscosity, surface tension and conductivity of the fluid.

Rutledge et al. developed a “whipping model” (Hohman et al., 2001a,b; Shin et al., 2001; Fridrikh et al., 2003) for the electrospinning process that mathematically describes the interaction between the electric field and fluid properties. They used this model to predict “terminal” jet diameter. The mathematically derived limiting diameter has been equated with experimentally measured fiber diameter. The key assumptions in the derivation of this “terminal” diameter include uniform electric field, no phase change and no inelastic stretching of the jet. Their model is qualitatively valid for selected polymeric solutions including polyethylene oxide (PEO) and polycaprolactone (PCL) in low concentrations (Hohman et al., 2001a).

Feng (2002) eliminated the ballooning instability of Rutledge model by including the effect of non-Newtonian extensional viscosity in electrospinning. Ying et al. (2005, 2006) conducted experiments to investigate the governing parameters in the electrospinning of PEO solution. Their findings showed that jet current has a positive correlation with PEO fibers confirming Rutledge model (Hohman et al., 2001a,b). Deitzel et al. (2001) evaluated the effect of spinning voltage and solution concentration on the morphology of polymeric nanofibers. Their experimental results revealed that solution concentration had a strong effect on fiber diameter. They

demonstrated that fiber diameter increases with increasing solution concentration according to a power law (power equal to 1/2). He et al. (2005) proposed an allometric relation for the current and flow rate that can be varied independently.

A number of investigators (McKee et al., 2004a,b; Gupta et al., 2005; Shenoy et al., 2005) have also looked into the rheological characteristics of the polymers to identify their effects on electrospinning. They specifically looked into the role of chain entanglement that seems to have a critical value dependent on the molecular weight and concentration. This “critical chain overlap concentration” can be theoretically estimated and experimentally determined (Gupta et al., 2005; Shenoy et al., 2005). These studies concluded that there is a dependence of fiber diameter on molecular weight and concentration, assumed to follow a power law (McKee et al., 2004a).

Recently, Helgeson and Wagner (2007) developed a correlation to predict fiber diameter for electrospinning process using dimensional analysis. Using Ohnesorge number and developing a new dimensionless group they were successful to develop a correlation that can be used to predict the fiber diameter a priori. Although this relation does not need knowledge of zero shear viscosity, it needs the value of conductivity that is significantly easier to measure than the viscosity. However, this empirical equation has one interesting limitation as observed by the authors. The proposed equation suggests that the fiber diameter does not depend on the fluid flow rate. This limits its application to laboratory experiments that assumes a “steady state operation”, rather than a manufacturing environment.

In summary, important progress has been made on the understanding of the electrospinning process resulting in multiple process models. However, these models still have conflicting requirements like surface tension or viscosity, inclusion or exclusion of fluid flow rate, allometric or isotropic relation, etc. Moreover, feed forward *ad hoc* control of the electrospinning process has shown ineffective controls resulting in wide variations in fiber diameters (Fong et al., 1999; Ying et al., 2005; Ying et al., 2006; Deitzel et al., 2001; He et al., 2005; McKee et al., 2004a). Both the temporal (millisecond operation) and spatial (sub-micron size) limitations make the process practically impossible to monitor in real time. As an

example, fiber diameters are typically measured off-line by a scanning electron microscope (SEM). This needs careful sample preparation implying time and forcing the process to be done off-line. Thus, to increase productivity and reduce cost, model-based feedback control of the electrospinning process is needed. This requires a computer model that can predict fiber diameter from process salient variables. Motivated by the success found in using neural networks to model non-linear process functions in various industries (Del Puerto and Ben Ghalia, 2002; Morquin et al., 2003; Liu, 1999), this paper proposes a neural network approach to predict the diameter of electro-spun nanofiber. As an example, this paper focuses on the modeling of electrospinning process for PEO aqueous solution. If successful, this method can be extended to other polymer solutions and has the potential to be adopted to explore a model-based feedback control scheme to regulate nanofiber diameter during manufacturing.

Most of the investigations covered here can be broadly divided into three areas, namely, closed form analytical models, rheological models, and dimensional analysis. Multiplicity of models and their attendant complexity are indicators of levels of nonlinearity and sensitivity of the suspected parameters and their interactions. Some of the proposed parameters are really not independent of each other either. As an example, concentration of a solution can be rather easily measured and controlled in a manufacturing environment. For a given polymer solution, they are typically controlled by the purity of the polymer, its molecular weight, quality of the solvent (DI water, as an example), and appropriate process control in making the solution. However, in existing models, concentration is typically not included as a model parameter. Rather, surface tension, conductivity, and zero shear viscosity are used in predicting fiber diameters. These parameters are difficult to measure, to say the least. More importantly, they are not independent of each other either. Thus, selecting the solution parameters to predict fiber diameter is rather challenging, particularly in a manufacturing environment.

From rheological approach, molecular weight or percent concentration are needed to predict “critical chain overlap”, and hence fiber diameter. Approximate solutions of analytical models approximate the effect of molecular weight for a given solution via the surface tension and do not explicitly include viscosity term. Dimensional analysis, however, includes both surface tension and conductivity. This model does not include viscosity term either. Given the complexity and limitations of various models discussed earlier, it was decided to develop a model that was useful in manufacturing environment. From experimental point of view, the easiest parameter to measure is conductivity. It is also relatively easy to control the concentration by controlling the quality of materials and flow of the process. Since PEO aqueous solution was one of the most studied system, this solution has been selected as a benchmark example in this paper.

The paper is organized as follows. Section 2 discusses the process parameters governing the electrospinning of PEO solution and presents quantitative measures of the effects of these parameters on the electro-spun fiber. Section 3 discusses the neural network predictive model. Network model selection and testing using the k -fold cross validation technique and computer simulation results are also presented. In Section 4, a

statistical study is presented to establish confidence intervals on the agreement between the experimental data and the data predicted by the neural network approach. Section 5 summarizes the findings of this paper and outlines some future work.

2. Process parameters

In electrospinning (Fig. 1), the fiber diameter depends on a number of parameters that may be divided into two groups, namely, *Intrinsic Parameters* and *Control Parameters*. *Intrinsic Parameters* (IP) are intrinsic properties of the fluid (molecular weight, relative permittivity, concentration, surface tension, viscosity, conductivity, etc.) and the environment (type, temperature, humidity, pressure/vacuum, etc.). *Control Parameters* (CP), in contrast, are the parameters that may be manipulated easily, even in real time in certain situations, in a manufacturing environment. Examples of control parameters include: applied electrical field, flow rate, distance between the nozzle and the collector, geometric details (shape, size, etc.) of the collector.

To model the electrospinning process, identification of certain process parameters like electric field strength and fluid flow rate is obvious. However, selection of other process parameters is not so obvious, or at least need some clarification. In this study, a qualitative model to select the process parameters is developed. This model takes advantage of both the “critical chain overlap” (McKee et al., 2004a,b; Gupta et al., 2005; Shenoy et al., 2005) and “jet instability” models (Hohman et al., 2001a,b; Shin et al., 2001; Fridrikh et al., 2003) discussed earlier. Based on the first model, concentration and molecular weight are identified as two process parameters that significantly influence the fiber diameter. According to this “critical chain overlap concentration” model, these parameters are covariants in the limit. In other words, the “overlap concentration” can be reached by changing either of these parameters and once this critical value is reached, fibers will be formed. Since surface tension for a given polymer solution depends on molecular weight and concentration, a process model should depend on these two parameters. If further “critical chain overlap” model is accepted, concentration alone is adequate to develop the model for a given polymeric solution. Solution concentration is the proposed third process parameter for this investigation.

Rutledge’s model (Hohman et al., 2001a,b; Shin et al., 2001; Fridrikh et al., 2003) also uses current through the fluid as an independent variable that is hard to measure. This current expectedly depends on the electrical behavior of the fluid and the imposed electrical field strength. The fluid current has two components, namely, conductive and advective currents. Conductive current depends on the conductivity (K) of the fluid. Advective current, on the other hand, depends on the fluid flow rate (Q) and space charge density. In electrospinning, space charge density is typically equated with surface charge density using the assumption of leaky dielectric fluid. In a leaky dielectric fluid model, as discussed earlier, most of the charges in the fluid accumulate on the surface rather than in the bulk of the fluid. In other words, advective current depends on fluid flow rate, applied field, and fluid behavior.

Table 1 – Reported experimental data for PEO nanofibers

Data index	Concentration (%)	Surface tension (mN/m)	Conductivity (mS/m)	Electrical field (V/cm)	Flow rate (cm ³ /min)	Nozzle diameter (mm)	Viscosity (cP)	Molecular weight (K)	Fiber diameter (nm)	Reference
1	1.0	77.8	3.27	700	0.01 ^{a*}	0.3	13	900	<80	Fong et al. (1999)
2	1.5	76.4	3.39	700	0.01 ^{a*}	0.3	32	900	80	Fong et al. (1999)
3	2.0	76.0	3.94	700	0.01 ^{a*}	0.3	74	900	100	Fong et al. (1999)
4	2.4	78.6	4.27	700	0.01 ^{a*}	0.3	160	900	150	Fong et al. (1999)
5	2.9	77.6	4.52	700	0.01 ^{a*}	0.3	289	900	180	Fong et al. (1999)
6	3.4	77.0	4.72	700	0.01 ^{a*}	0.3	527	900	200	Fong et al. (1999)
7	3.8	76.6	4.90	700	0.01 ^{a*}	0.3	1250	900	250	Fong et al. (1999)
8	4.3	76.2	5.13	700	0.01 ^{a*}	0.3	1835	900	250	Fong et al. (1999)
9	7.0	44.0	9.7 ^b	424	0.016	0.35	3800	400	250	Deitzel et al. (2001)
10	10.0	38.0	10.0 ^b	424	0.016	0.35	20000	400	400	Deitzel et al. (2001)
11	5.0	75.9	11.3	375	0.00333	0.6	2000 ^d	500	540	Ying et al. (2005, 2006)
12	5.0	75.9	11.3	500	0.00333	0.6	2000 ^d	500	523	Ying et al. (2005, 2006)
13	5.0	75.9	11.3	750	0.00333	0.6	2000 ^d	500	444	Ying et al. (2005, 2006)
14	2.52	78.6 ^c	7.8	1538	0.05	0.84 ^{a**}	180	900	84	Daga et al. (2006)
15	3.74	77 ^c	10.1	1538	0.05	0.84 ^{a**}	910	900	133	Daga et al. (2006)
16	4.5	76.2 ^c	10.8	1538	0.05	0.84 ^{a**}	2650	900	153	Daga et al. (2006)
17	5.5	75.6 ^c	11.8	1538	0.05	0.84 ^{a**}	6440	900	178	Daga et al. (2006)
18	6.5	75.1 ^c	12.8	1538	0.05	0.84 ^{a**}	15600	900	191	Daga et al. (2006)

Notes:

^{a*}Fluid flow rate measurements for Data #1–8 were obtained from a private communication with the authors.

^{a**}Nozzle diameter for Data #14–18 is obtained from a private communication with the authors.

^bConductivity data for Data #9–10 are obtained through measurements conducted the authors for PEO with molecular weight equal to 900,000. Conductivity Data #11–13 are based on Daga et al. (2006) and Saboormaleki et al. (2004).

^cSurface tension values for Data #14–18 were estimated from data given in references (Fong et al., 1999; Deitzel et al., 2001).

^dViscosity values for Data #11–13 were estimated using extrapolation of known data.

Since, electric field strength and fluid flow rates are already selected as two input parameters, it is believed that inclusion of conductivity as a process parameter should be appropriate.

Importance of conductivity has also been noted by Feng (2002). A higher conductivity causes the surface charge to move faster towards the collector electrode resulting in reduced surface charge. Since solvent plays an important role in this process and typically accounts for 90% or more of the solution, it is important to include its effect. In electrospinning, polymer is the solute and the solvent is typically DI (de-ionized) water. Typical conductivity (ELGA Labwater, 2008) of DI water varies between 0.1 and 0.01 (mS/m). This difference in conductivity of the solvent may contribute significantly to the conductivity of the polymer solution. Based on these observations, the conductivity is used as the fourth and final independent variable for this model.

Literature survey was conducted to compile all the relevant process parameters for aqueous PEO solutions. Data was collected from 19-independent researchers in five different institutions over a 7-year period (1999–2006) (Fong et al., 1999; Ying et al., 2005; Ying et al., 2006; Deitzel et al., 2001; Daga et al., 2006). The collected data is reported in Table 1. As expected, some important data was missing in original papers. To complete the table, other means like personal communications, additional in-house experiment, and interpolation of reported data were also used. One interesting observation was about the independence of fiber diameter from the nozzle diameter. Even if the nozzle diameter varied significantly (0.025–0.84 mm, it was not usually reported or discussed in these investigations. Part of the reason is the fact that fiber diameters are typically four orders of magnitude smaller than the nozzle diameters and whatever effect it has is mostly limited to the local region near the opening of the nozzle. As the jet moves away from the nozzle and other physical phenomena like instability, stretching, evaporation, take over, the nozzle diameter has lesser and lesser effect. Consequently, it is believed that fiber diameter depends only on two sets of parameters (intrinsic and control) discussed earlier and adequately represented by the four input variables used in the proposed model.

Table 1 shows the range of solution concentrations (%), electric field strength (V/cm), and fluid flow rate (cm³/min) for aqueous PEO data. It also shows the range of fiber diameters (nm) measured under these conditions. Apart from the key information (concentration, electrical field, and fluid rate), Table 1 also contains other related information like surface tension (mN/m) and conductivity (μS/m), viscosity (cP), relative permittivity, and molecular weight. Electric field strength (V/cm) is calculated by dividing the applied voltage (V) with the distance (cm) between the spinneret and the collector. Data is arranged in groups of different references in increasing concentrations.

It may be noted that amount of PEO has been used to calculate concentration of PEO from the data given in reference (Fong et al., 1999) and reported in Table 1. As a result, concentration used in Table 1 is slightly lower than the amount of PEO given in the Reference. It may also be noted that even if the concentration has changed (Fong et al., 1999) (Data # 1 through 8 in Table 1) more than four times (1–4.3%), surface tension effectively remains the same (about 77 mN/m). Fiber

Table 2 – List of input variables that have high influence on the diameter of the electro-spun fiber

Independent input variables	Description
$x_1 = C$	Solution concentration
$x_2 = K$	Conductivity
$x_3 = E$	Electric field strength
$x_4 = Q$	Flow rate

diameter has, however, increased more than three times (less than 80–250 nm) under these conditions.

It is important to make a few observations on the data in Table 1 based on earlier discussions. About three fourth of the data were for a molecular weight of 900 K. Consequently, focus of the investigation has been on the wide range of values for concentrations, rather than the effect of molecular weight. Under this constraint, concentration is adequate to identify all independent variables of “critical chain overlap.” For a given concentration, surface tension, viscosity, and conductivity are all interdependent for aqueous PEO solutions. Due to the difficulty in measuring certain parameters like surface tension and zero shear viscosity, it is reasonable to use interdependency of fluid properties to select appropriate process parameters. Based on these observations, it was decided to use the four measurable and controllable process parameters, namely concentration, conductivity, electric field strength and flow rate, as the input variables to the neural network model. These variables are summarized in Table 2.

Let

$$X = [x_1, x_2, x_3, x_4]^T = [C, K, E, Q]^T \quad (1)$$

be the input vector of independent variables that have high influence on the diameter of the fiber formed by the electrospinning process. The measured fiber diameter, d , is assumed to be given by

$$d = F(X) + \varepsilon \quad (2)$$

where $F(\cdot)$ is the true “unknown” function that relates the input variables to the fiber diameter variable, and ε is a zero-mean random noise term assumed to have a finite variance. The objective of this paper is to develop a neural network model that can approximate the function $F(X)$. The neural network model can then be used to predict fiber diameter for various admissible sets of values for the input variables. PEO aqueous solution was used as the bench mark material to investigate the viability of neural network as a tool for predicting fiber diameter.

3. Neural network predictive model

In this study, the variable of interest is the fiber diameter which represents the output variable of the electrospinning process. Neural networks have been shown to be capable of building a class of very flexible models (White, 1992; Nielson, 1990) which can be used for a variety of different applications, such as non-linear regression and discrimination analysis (Del Puerto and Ben Ghalia, 2002; Morquin et al., 2003; Liu, 1999; Patel et al.,

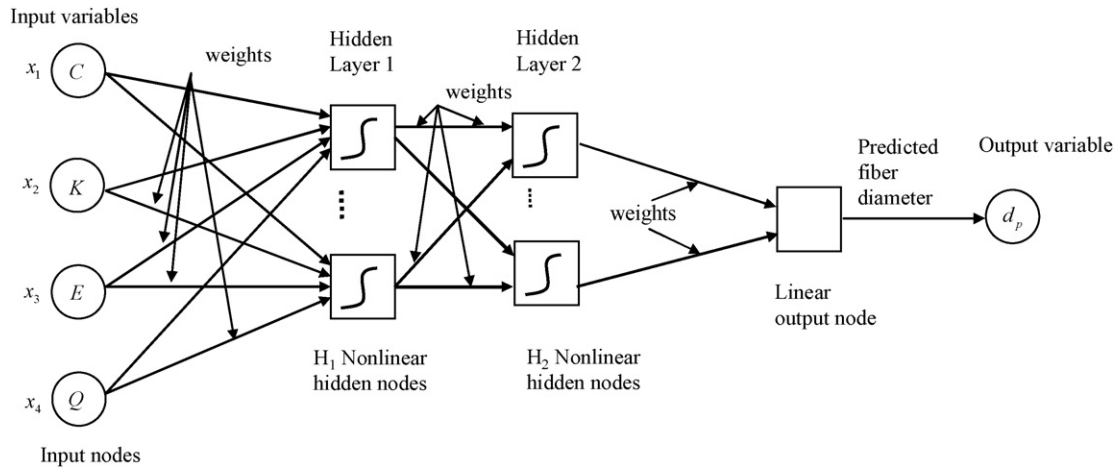


Fig. 2 – Proposed multilayer perceptron neural network for fiber diameter prediction.

2006). Different types of neural networks have been proposed. In this study, a predictive model built using a multilayer perceptron (MLP) network (White, 1992) is proposed. Fig. 2 shows the structure of the proposed MLP network. The goal of neural network modeling is to predict the fiber diameter using a function of the inputs, which are measurable variables that act upon the output. A desirable network architecture contains as few hidden layers and as few hidden nodes for a good prediction of the fiber diameter. In this study, it was found that a network with two hidden layers provided a good prediction performance. The use of one single hidden layer led to poor performance no matter how many hidden nodes were added to the network, indicating highly nonlinear mapping in the process. The network output, d_p , is the predicted fiber diameter which can be expressed by a function $f(X, w)$ of the input data $X = [x_1, x_2, x_3, x_4]^T$ and the network parameters w commonly called weights.

The neural network output is given by

$$d_p = f(X, w) = \sum_{h_2=1}^{H_2} \lambda_{h_2} g \left(\sum_{h_1=1}^{H_1} \beta_{h_2 h_1} g \left(\sum_{i=1}^4 \gamma_{h_1 i} x_i \right) \right) \quad (3)$$

with network weight vector $w = [\lambda_1, \dots, \lambda_{H_2}, \beta_{11}, \dots, \beta_{H_2 H_1}, \gamma_{11}, \dots, \gamma_{H_1 4}]^T$. The scalars H_1 and H_2 denote the number of nodes in hidden layers 1 and 2 of the network, respectively, and $g(\cdot)$ is a nonlinear activation function attached to each hidden node. The function $g(\cdot)$ is selected to be the hyperbolic tangent function. Considering Eqs. (2) and (3), the neural network can be interpreted as a parametric nonlinear regression of d on X . The network model is completely determined once the number of nodes in hidden layers 1 and 2 have been determined and the network weights have been calculated. The training–testing method for the neural network model is discussed next.

3.1. Network training and testing using k -fold cross validation

The dataset available in Table 1 represents a finite-sized sample set from a population with an unknown probability

distribution. The traditional method for training and testing a neural network model calls for splitting the dataset into a training subset and a testing subset. The training data subset is used to calculate the weights of the network and the test data subset is used to assess the performance of the network. When the size of the available data is small, the simple training–test data splitting method is not effective. Even with a large size data, the performance of the neural network cannot be estimated on all future samples presented to the network if a simple training–test data splitting method is used. This is clearly impossible unless the underlying probability distribution that the training samples are drawn from is exactly equal to the probability distribution from which the future samples are drawn.

There are a number of schemes for addressing this problem and the most suitable for the size of dataset used in this study, is k -fold cross validation (Kohavi, 1995) (KCV). This technique randomly divides the available data into k equal size and mutually exclusive partitions (or folds). For a k -fold cross validation k neural networks are trained with a different fold used each time as the test set, while the other $k - 1$ folds are used for the training data. The choice of k influences the ratio of data used for training and testing with an optimal value of k in the range 5–10. The performance obtained using a KCV procedure is less biased than the one obtained using a simple training–test data splitting method (Kohavi, 1995).

The KCV procedure requires that the number of data samples is a multiple of the number of folds. Sixfold cross validation was used in this study. The available data was randomly partitioned into six mutually exclusive groups. These partitions were combined according to the KCV procedure into six training and test partition pairs as shown in Table 3. The partition pairs were used to train six neural network models. Fig. 3 illustrates the implemented six-cross validation procedure.

The number of hidden layers and the number of nodes per hidden layer in the neural network architecture were determined experimentally. It was concluded from the study that the minimal network architecture for the fiber diameter prediction problem consists of two hidden layers with 12 nodes in the first hidden layer ($H_1 = 12$) and 7 nodes in the second hidden layer ($H_2 = 7$). All the six network models have the

Table 3 – Training–testing partition pairs using sixfold cross validation procedure

Partition pair index	Training set	Test set
1	Partition {1,2,3,4,5}	Partition {6}
2	Partition {1,2,3,4,6}	Partition {5}
3	Partition {1,2,3,5,6}	Partition {4}
4	Partition {1,2,4,5,6}	Partition {3}
5	Partition {1,3,4,5,6}	Partition {2}
6	Partition {2,3,4,5,6}	Partition {1}

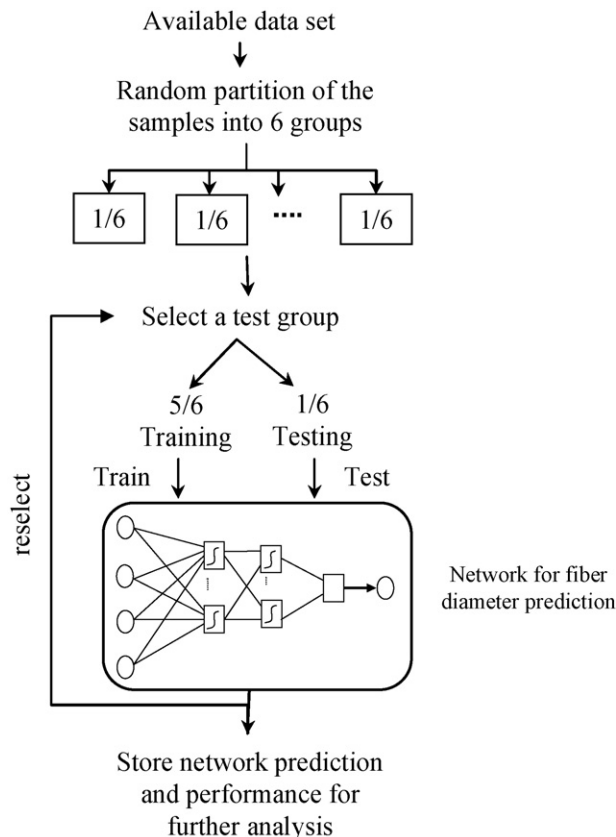
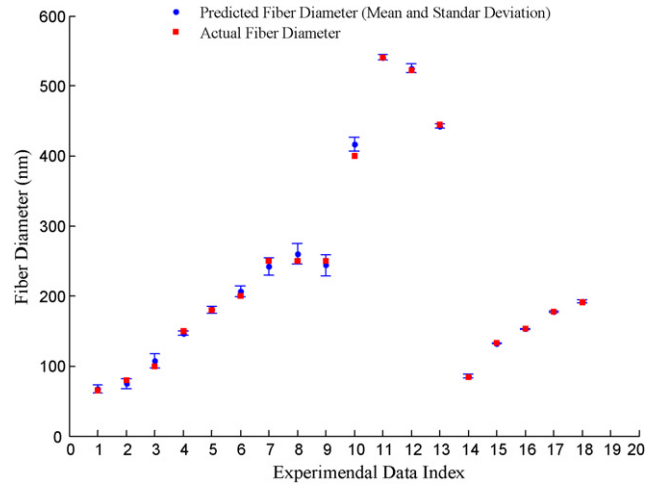
same architecture but differ by the values for their network connection weight vectors w . The network weights were calculated iteratively using the MATLAB Neural Network Toolbox (Demuth et al., 2006).

3.2. Simulation results

The mean squared prediction error is calculated for each network as

$$\text{MSPE}_n = \frac{100}{N_{\text{te}} \sigma_{dn}^2} \sum_{i=1}^{N_{\text{te}}} (d_n(i) - d_{pn}(i))^2, \quad n = 1, \dots, 6 \quad (4)$$

where d_n is the vector of actual fiber diameter values used during the testing of network n , d_{pn} is the vector of fiber diameter values predicted by network n , σ_{dn}^2 is the variance of d_n , and $N_{\text{te}} = 3$ is the number of data used for network testing. The

**Fig. 3 – Neural network training and testing using sixfold cross validation procedure.****Fig. 4 – Network prediction results (cross validation mean and standard deviation).**

cross validation error (CVE) is defined as

$$\text{CVE} = \frac{1}{6} \sum_{n=1}^6 \text{MSPE}_n \quad (5)$$

The network architecture with two hidden layers and 19 hidden nodes ($H_1 = 12$ and $H_2 = 7$) resulted in the lowest cross validation error percentage of 6.81%. This means that the cross validation prediction accuracy percentage, given by $100(1 - \text{CVE})$, is equal to 93.19%. This indicates a high prediction performance of the six network models on average. Before concluding whether or not a neural network approach is viable for fiber diameter prediction, the prediction standard deviation should also be calculated. The six network models were tested during a second phase on all available dataset. The average and standard deviation of predictions were calculated and the results were reported in Fig. 4. It can be seen that on average the network models provide very good predictions for all samples. In addition, the prediction standard deviations are small enough to be able to conclude that the developed neural network approach is a viable method for fiber diameter prediction. Fig. 5 shows the correlation between the actual fiber diameter data and the average predictions from all the six network models.

Let d_{pn} be the prediction vector by network n , $n = 1, \dots, 6$, and let $d_p = 1/6 \sum_{n=1}^6 d_{pn}$ be the average prediction vector. The correlation coefficient between the actual fiber diameter data and the prediction results is given by

$$r = \sqrt{1 - \frac{\sum_{i=1}^N (d(i) - d_p(i))^2}{\sum_{i=1}^N (d(i) - \bar{d})^2}} \quad (6)$$

where \bar{d} is the mean of actual fiber diameter data vector and N is the size of the available dataset ($N = 18$). The correlation coefficient measures the strength of the relation between the actual fiber diameter variable d and the predicted fiber diameter variable d_p . Using the cross-validation method, $r = 0.9992$ which indicates a high correlation. The least-square

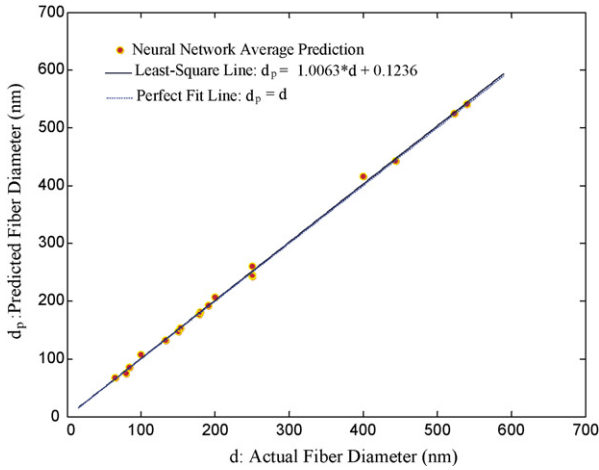


Fig. 5 – Correlation between predicted nanofiber diameter and actual data.

regression line (Fig. 5) is given by $d_p = 1.0063d + 0.1236$. This also indicates a strong agreement between the actual data and the predicted results. However, because of the limited size of the dataset further statistical analysis is needed to build some confidence intervals on the correlation between the actual data and the predicted data. This is the subject of the next section.

4. Statistical analysis of the network prediction

The objective of this section is to calculate confidence intervals on the agreement between the experimental method

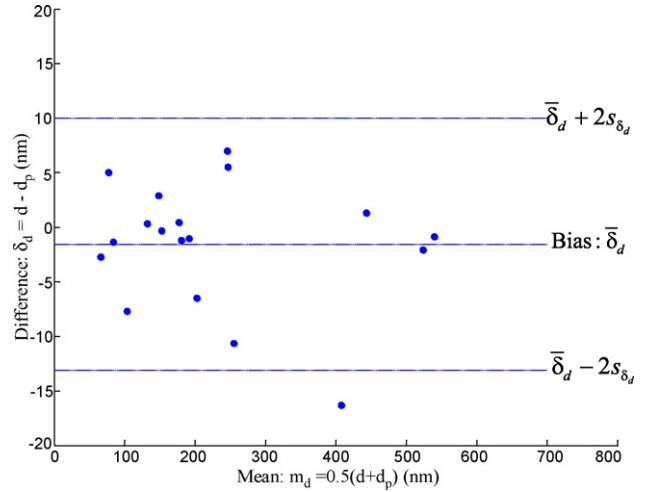


Fig. 6 – Difference between the actual data and the predicted data against their mean values.

and the neural network method. Let $\delta_d = d - d_p$ be the difference between the actual data obtained by the experimental method and the predicted data obtained by the neural network method. The variable δ_d is the prediction error. Let $m_d = (1/2)(d + d_p)$ be their mean. Fig. 6 shows the graph of the difference between the actual data and the predicted data against their mean values. This graph is more useful when comparing two methods (Altman and Bland, 1983). The degree of agreement between the two methods is quantified by the bias, estimated by the mean difference $\bar{\delta}_d$ and the standard deviation of the difference s_{δ_d} . The mean difference is equal to $\bar{\delta}_d = -1.5728$ (nm) and the standard deviation $s_{\delta_d} = 5.7741$ (nm). It

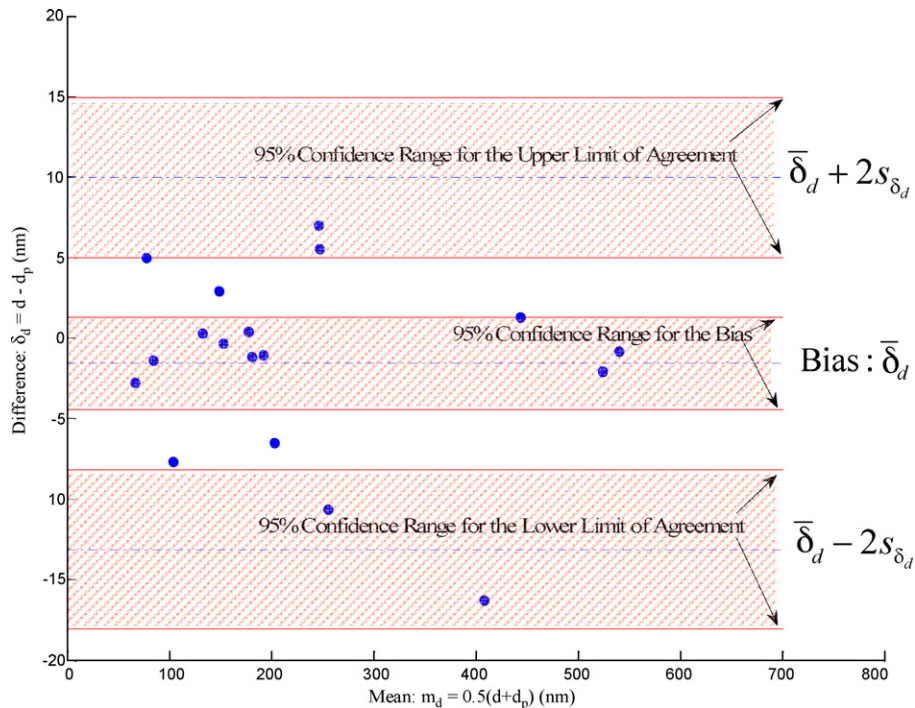


Fig. 7 – The 95% confidence intervals for the bias and the limits of agreements between the experimental data and the neural network predicted data.

is expected that most of the differences to lie between $\bar{\delta}_d - 2s_{\delta_d}$ and $\bar{\delta}_d + 2s_{\delta_d}$ referred to as the limits of agreements (Altman and Bland, 1983). If the differences are normally distributed, 95% of the differences will lie between these limits (Altman and Bland, 1983). The lower limit of agreement is equal to $\bar{\delta}_d - 2s_{\delta_d} = -13.1210$ (nm) and the upper limit of agreement is equal to $\bar{\delta}_d + 2s_{\delta_d} = 9.9754$ (nm). Fig. 6 shows the lower and the upper limits of agreement. It can be seen that most of the difference lie between these limits. The predicted data may be about 13 (nm) above or about 10 (nm) below the actual data. These limits are small enough to suggest a good agreement between the predicted data and actual experimental data.

The limits of agreement are only estimates and do not represent the true values which apply to the whole population. A different dataset would give different limits. Thus, it is important to use standard errors and confidence intervals to see how precise the estimates are. The standard errors of $\bar{\delta}_d$ is $\sqrt{s_{\delta_d}^2/N}$ where N is the sample size, and the standard error of $\bar{\delta}_d - 2s_{\delta_d}$ and $\bar{\delta}_d + 2s_{\delta_d}$ is $\sqrt{3s_{\delta_d}^2/N}$ (Altman and Bland, 1983). The 95% confidence intervals can be calculated by finding the appropriate value of the t-distribution with $N - 1$ degrees of freedom (Harnett, 1982; Volk, 1969) (risk level $\alpha = 5\% = 0.05$ and $N - 1 = 17$). The t-value could be obtained from t-distribution tables that are available in many basic statistics books such as references (Harnett, 1982; Volk, 1969). The t-value is found to be equal to $t_{0.05,17} = 2.110$ (Volk, 1969, Table 6.1).

The 95% confidence interval for the bias is given by $\bar{\delta}_d \pm t_{0.05,N-1} \sqrt{s_{\delta_d}^2/N}$, giving a range between -4.445 and 1.2989 (nm). The 95% confidence interval for the limit of agreement is given by $s_{\delta_d} \pm t_{0.05,N-1} \sqrt{3s_{\delta_d}^2/N}$, giving a range between -18.0949 and -8.1471 (nm) for the lower limit and a range between 5.0015 and 14.9493 (nm) for the upper limit. The 95% confidence intervals for the bias and the limits of agreements are graphed in Fig. 7. These intervals are narrow which reflect a high confidence in using the neural network approach for the prediction of nanofiber diameter.

5. Conclusion

This paper investigates the viability of neural network as a tool for predicting the diameter of nanofiber formed by an electrospinning process. Concentration, conductivity, flow rate, and electric field strength have been shown to have high influence on fiber diameter. These salient parameters are used as the input variables to the neural network model. Experimental dataset for polyethylene oxide (PEO) aqueous solution were used to train and test the neural network model. Network model selection, training and testing were conducted using the k-fold cross validation technique which was demonstrated to be the most suitable scheme for the size of the experimental dataset. Sixfold cross validation was used in this study. The designed six neural network models were simulated and their mean predictions and standard deviations were calculated. The simulations results show high correlation between the experimental data and the mean predictions. The standard deviations on all network predictions were small, indicating consistency (low vari-

ation) in the prediction performances of the six network models.

Further analysis of the performance of the neural network approach was conducted using statistical methods. 95% confidence intervals were calculated for the bias and the lower and upper limits of agreement between the experimental data and the neural network predicted data. The calculated confidence intervals are narrow, implying a high confidence in using the neural network approach for the prediction of nanofiber diameter.

While the proposed neural network approach is not intended to model the complete complex physics of the electrospinning process, the results of this study demonstrated the viability of the neural network approach as a promising tool for predicting nanofiber diameter. PEO aqueous solution was used as the benchmark material in this study. Future work will consider applying the method developed in this study to other types of solutions. Because open-loop control of the electrospinning process often results in wide variations in fiber diameters, a neural network model-based feedback control technique to regulate nanofiber diameter is worth exploring.

Acknowledgements

Authors are thankful to Drs. James Li and Jaime Ramos, the University of Texas-Pan American, Dr. Sureeporn Tripatanasuwan, Polymer Science Group of Prof. Darrell Reneker, University of Akron, Akron, Ohio, Prof. Norman Wagner, University of Delaware, and Mr. Sang Hoon Lee, Mechanical Engineering Department, University of California, Berkeley, for their help at various stages of the project including validation of some critical information used in Table 1, and the anonymous referees for their helpful comments.

REFERENCES

- Reneker, D.H., Fong, H., 2006. Polymeric nanofibers, ACS Symposium Series 918. American Chemical Society.
- Altman, D.G., Bland, J.M., 1983. Measurement in medicine: the analysis of method comparison studies. *The Statistician* 32, 307–317.
- Daga, V.K., Helgeson, M.E., Wagner, N.J., 2006. Electrospinning of neat and laponite-filled aqueous poly(ethylene oxide) solutions. *Journal of Polymer Science: Part B: Polymer Physics* 44, 1608–1617.
- Deitzel, J.M., Kleinmeyer, J.D., Hirvonen, J.K., Beck Tan, N.C., 2001. The effect of processing variables on the morphology of electrospun nanofibers and textiles. *Polymer* 42, 261–272.
- Del Puerto, F., Ben Ghalia, M., 2002. White color tracking adjustment in television receivers using neural networks. *Engineering Applications of Artificial Intelligence* 15, 601–606.
- ELGA Labwater, 2008. Weblink: <http://www.elgalabwater.com/?id=503>.
- Feng, J.J., November 2002. The stretching of an electrified non-Newtonian jet: a model for electrospinning. *Physics of Fluids* 14 (11), 3912–3926.
- Fong, H., Chun, I., Reneker, D.H., 1999. Beaded nanofibers formed during electrospinning. *Polymer* 40, 4585–4592.

- Fridrikh, S.V., Yu, J.H., Brenner, M.P., Rutledge, G.C., 2003. Controlling the fiber diameter during electrospinning. *Physical Review Letters* 90 (April (14)), 144502-1–144502-4.
- Gupta, P., Elkins, C., Long, T.E., Wilkes, G.L., 2005. Electrospinning of linear homopolymers of poly(methyl methacrylate): exploring relationships between fiber formation, viscosity, molecular weight and concentration in a good solvent. *Polymer* 46 (April) (online 20 pages).
- Harnett, D., 1982. *Statistical Methods*, 3rd ed. Addison-Wesley.
- He, J.H., Wan, Y.Q., Yu, J.Y., 2005. Scaling law in electrospinning: relationship between electric current and solution flow rate. *Journal of Polymer* 46, 2799–2801.
- Helgeson, M.E., Wagner, N.J., 2007. A correlation for the diameter of electrospun polymer nanofibers. *American Institute of Chemical Journal* 53 (1), 51–55.
- Hohman, M.M., Shin, M., Rutledge, G.C., Brenner, M.P., 2001a. Electrospinning and electrically forced liquid jets. I. Stability theory 2001. *Physics of Fluids* 13 (8), 2201–2220.
- Hohman, M.M., Shin, M., Rutledge, G.C., Brenner, M.P., 2001b. Electrospinning and electrically forced liquid jets: II. Applications *Physics of Fluids* 13 (8), 2221–2236.
- Kohavi, R., 1995. A study of cross validation and bootstrap for accuracy estimation and model selection. In: *Proceedings of the 14th International Joint Conference on Artificial Intelligence*, pp. 1137–1143.
- Liu, Y., 1999. Neural network based adaptive control and optimisation in the milling process. *International Journal of Advanced Manufacturing Technology* 15, 791–795.
- McKee, M.G., Wilkes, G.L., Colby, R.H., Long, T.E., 2004a. Correlations of solution rheology with electrospun fiber formation of linear and branched. *Polyesters Macromolecules* 37 (5), 1760–1767.
- McKee, M.G., Elkins, C.L., Long, T.E., 2004b. Influence of self-complementary hydrogen bonding on solution rheology/electrospinning relationships. *Polymer* 45 (26), 8705–8715.
- Melcher, J.R., Taylor, G.I., 1969. Electrohydrodynamics: a review of the role of interfacial shear stresses. *Annual Review of Fluid Mechanics* 1 (1), 111–146.
- Morquin, D., Ben Ghalia, M., Bose, S., 2003. An integrated neural network-based vision system for automated separation of clods from agricultural produce. *Engineering Applications of Artificial Intelligence* 16, 45–55.
- Demuth, H., Beale, M., Hagan, M., 2006. *Neural Network Toolbox 5 for Use with MATLAB*, Mathworks, Inc.
- Nielson, H., 1990. *Neural Computing*. Addison-Wesley, MA, pp. 89–93.
- Patel, S.U., Kumar, B.J., Badhe, Y.P., Sharma, B.K., Saha, S., Biswas, S., Chaudhury, A., Tambe, S.S., Kulkarni, B.D., 2006. Estimation of gross calorific value of coals using artificial neural networks. *Fuel* 86, 334–344.
- Reneker, D.H., Yarin, A., Fong, L., Koombhongse, H., Bending, S., 2000. instability of electrically charged liquid jets of polymer solutions in electrospinning. *Journal of Applied Physics* 87 (9), 4531–4547.
- Saboormaleki, M., Barnes, A.R., Schlindwein, W.S., 2004. Characterization of polyethylene oxide (PEO) based polymer electrolytes. *The Electrochemical Society (Abstract 725, 205th Meeting)*.
- Saville, D.A., 1970. Electrohydrodynamic stability: fluid cylinders in longitudinal electric fields. *Physics of Fluids* 13 (12), 2987–2994.
- Saville, D.A., 1971. Electrohydrodynamic stability: effects of charge relaxation on the interface of a liquid jet. *Journal of Fluid Mechanics* 48, 815–827.
- Saville, D.A., 1997. Electrohydrodynamics: the Taylor–Melcher leaky dielectric model. *Annual Review of Fluid Mechanics* 29, 27–64.
- Shenoy, S., Douglas Bates, W., Frisch, H.L., Wnek, G.E., 2005. Role of chain entanglement on fiber formation during electrospinning of polymer solutions: good solvent, non-specific polymer–polymer interaction limit. *Polymer* 46 (March) (online 25 pages).
- Shin, M., Hohman, M.M., Brenner, M.P., 2001. Rutledge GC electrospinning: a whipping fluid jet generates submicron polymer fibers. *Applied Physics Letters* 78 (8), 1149–1151.
- Taylor, G.I., 1964. Disintegration of water drops in an electric field. *Proceedings of Royal Society of London* 280 (1382), 383–397.
- Taylor, G.I., 1966. Studies in electrohydrodynamics. I. The circulation produced in a drop by an electric field. *Proceedings of Royal Society of London* 291 (1425), 159–166.
- Taylor, G.I., 1969. Electrically driven jets. *Proceedings of Royal Society of London* 313 (A), 453–475.
- Volk, W., 1969. *Applied Statistics for Engineers*, 2nd ed. McGraw-Hill, pp. 109–148.
- White, H., 1992. *Artificial Neural Networks: Approximation and Learning Theory*. Blackwell Publishers, Cambridge, MA.
- Ying, Y., Zhidong, J., Qiang, L., Zhicheng, G., 2005. Controlling the electrospinning process by jet current and Taylor Cone. In: *2005 Annual Report Conference on Electrical Insulation and Dielectric Phenomena*, pp. 453–456.
- Ying, Y., Zhidong, J., Qiang, L., Zhicheng, G., 2006. Experimental investigation of the governing parameters in the electrospinning of polyethylene oxide solution. *IEEE Transactions on Dielectrics and Electrical Insulation* 13, 485–580.